



## OPEN ACCESS

## EDITED BY

Takaji Matsutani,  
Maruho, Japan

## REVIEWED BY

Dwijendra K. Gupta,  
Allahabad University, India  
Peng Li,  
Max Planck Institute for Demographic  
Research, Germany

## \*CORRESPONDENCE

Muneyuki Masuda

✉ mmuneyuki@icloud.com;

✉ masuda.muneyuki.pg@mail.hosp.go.jp

RECEIVED 14 July 2024

ACCEPTED 13 December 2024

PUBLISHED 10 January 2025


## CITATION

Sato K, Toh S, Murakami T, Nakano T, Hongo T, Matsuo M, Hashimoto K, Sugasawa M, Yamazaki K, Ueki Y, Nakashima T, Uryu H, Ono T, Umeno H, Ueda T, Kano S, Tsukahara K, Watanabe A, Ota I, Monden N, Iwae S, Maruo T, Asada Y, Hanai N, Sano D, Ozawa H, Asakage T, Fukusumi T and Masuda M (2025) Nationwide multi-centric prospective study for the identification of biomarkers to predict the treatment responses of nivolumab through comprehensive analyses of pretreatment plasma exosome mRNAs from head and neck cancer patients (BIONEXT study). *Front. Immunol.* 15:1464419. doi: 10.3389/fimmu.2024.1464419

## COPYRIGHT

© 2025 Sato, Toh, Murakami, Nakano, Hongo, Matsuo, Hashimoto, Sugasawa, Yamazaki, Ueki, Nakashima, Uryu, Ono, Umeno, Ueda, Kano, Tsukahara, Watanabe, Ota, Monden, Iwae, Maruo, Asada, Hanai, Sano, Ozawa, Asakage, Fukusumi and Masuda. This is an open-access article distributed under the terms of the [Creative Commons Attribution License \(CC BY\)](https://creativecommons.org/licenses/by/4.0/). The use, distribution or reproduction in other forums is permitted, provided the original author(s) and the copyright owner(s) are credited and that the original publication in this journal is cited, in accordance with accepted academic practice. No use, distribution or reproduction is permitted which does not comply with these terms.

# Nationwide multi-centric prospective study for the identification of biomarkers to predict the treatment responses of nivolumab through comprehensive analyses of pretreatment plasma exosome mRNAs from head and neck cancer patients (BIONEXT study)

Kuniaki Sato<sup>1</sup>, Satoshi Toh<sup>1</sup>, Taku Murakami<sup>2</sup>, Takafumi Nakano<sup>1</sup>, Takahiro Hongo<sup>1</sup>, Mioko Matsuo<sup>3</sup>, Kazuki Hashimoto<sup>3</sup>, Masashi Sugasawa<sup>4</sup>, Keisuke Yamazaki<sup>5</sup>, Yushi Ueki<sup>5</sup>, Torahiko Nakashima<sup>6</sup>, Hideoki Uryu<sup>6</sup>, Takeharu Ono<sup>7</sup>, Hirohito Umeno<sup>7</sup>, Tsutomu Ueda<sup>8</sup>, Satoshi Kano<sup>9</sup>, Kiyooki Tsukahara<sup>10</sup>, Akihito Watanabe<sup>11</sup>, Ichiro Ota<sup>12</sup>, Nobuya Monden<sup>13</sup>, Shigemichi Iwae<sup>14</sup>, Takashi Maruo<sup>15</sup>, Yukinori Asada<sup>16</sup>, Nobuhiro Hanai<sup>17</sup>, Daisuke Sano<sup>18</sup>, Hiroyuki Ozawa<sup>19</sup>, Takahiro Asakage<sup>20</sup>, Takahito Fukusumi<sup>21</sup> and Muneyuki Masuda <sup>1\*</sup>

<sup>1</sup>Department of Head and Neck Surgery, National Hospital Organization Kyushu Cancer Center, Fukuoka, Fukuoka, Japan, <sup>2</sup>Showa Denko Materials America, R&D Center, Irvine, CA, United States,

<sup>3</sup>Department of Otolaryngology, Head and Neck Surgery, Graduate School of Medical Science, Kyushu University, Fukuoka, Fukuoka, Japan, <sup>4</sup>Department of Head & Neck Surgery, International Medical Center, Saitama Medical University, Hidaka, Saitama, Japan, <sup>5</sup>Department of Otolaryngology, Head and Neck Surgery, Niigata University Graduate School of Medical and Dental Sciences, Niigata, Niigata, Japan, <sup>6</sup>Department of Otorhinolaryngology, National Hospital Organization Kyushu Medical Center, Fukuoka, Fukuoka, Japan, <sup>7</sup>Department of Otolaryngology, Head and Neck Surgery, Kurume University School of Medicine, Kurume, Fukuoka, Japan, <sup>8</sup>Department of Otorhinolaryngology, Head and Neck Surgery Graduate School of Biomedical and Health Sciences Hiroshima University, Hiroshima, Hiroshima, Japan, <sup>9</sup>Department of Otolaryngology, Head and Neck Surgery, Faculty of Medicine and Graduate School of Medicine, Hokkaido University, Sapporo, Hokkaido, Japan, <sup>10</sup>Department of Otorhinolaryngology, Head and Neck Surgery, Tokyo Medical University, Tokyo, Japan, <sup>11</sup>Department of Otolaryngology, Head and Neck Surgery, Keiyukai Sapporo Hospital, Sapporo, Hokkaido, Japan, <sup>12</sup>Department of Otolaryngology-Head and Neck Surgery, Nara Medical University, Kashihara, Nara, Japan, <sup>13</sup>Department of Head and Neck Surgery, National Hospital Organization Shikoku Cancer Center, Matsuyama, Ehime, Japan, <sup>14</sup>Department of Head and Neck Surgery, Hyogo Cancer Center, Akashi, Hyogo, Japan, <sup>15</sup>Department of Otorhinolaryngology, Nagoya University Graduate School of Medicine, Nagoya, Aichi, Japan, <sup>16</sup>Department of Head and Neck Surgery, Miyagi Cancer Center, Natori, Miyagi, Japan, <sup>17</sup>Department of Head and Neck Surgery, Aichi Cancer Center Hospital, Nagoya, Aichi, Japan, <sup>18</sup>Department of Otorhinolaryngology-Head and Neck Surgery, School of Medicine, Yokohama City University, Yokohama, Kanagawa, Japan, <sup>19</sup>Keio University School of Medicine, Otolaryngology, Head and Neck Surgery, Tokyo, Japan, <sup>20</sup>Department of Head and Neck Surgery, Tokyo Medical and Dental University, Tokyo, Japan, <sup>21</sup>Department of Otorhinolaryngology-Head and Neck Surgery, Osaka University Graduate School of Medicine, Suita, Osaka, Japan

**Background:** Nivolumab paved a new way in the treatment of patients with recurrent or metastatic (RM) head and neck squamous cell carcinoma (RM-HNSCC). However, the limited rates of long-term survivors (< 20%) demand a robust prognostic biomarker. This nationwide multi-centric prospective study aimed to identify a plasma exosome (PEX) mRNA signature, which serves as a companion diagnostic of nivolumab and provides a biological clue to develop effective therapies for a majority of non-survivors.

**Methods:** Pre-treatment plasmas ( $N = 104$ ) of RM-HNSCC patients were subjected to comprehensive PEX mRNA analyses for prognostic marker discovery and validation. In parallel, paired treatment-naïve tumor and plasma samples ( $N = 20$ ) were assayed to elucidate biological implications of the PEX mRNA signature.

**Results:** Assays for pre-treatment blood samples ( $N = 104$ ) demonstrated that a combination of 6 candidate PEX mRNAs plus neutrophil-to-lymphocyte ratio precisely distinguished non-survivors from >2-year survivors (2-year OS; 0% vs 57.7%;  $P = 0.000124$ ) with a high hazard ratio of 2.878 (95% CI 1.639-5.055;  $P = 0.0002348$ ). Parallel biological assays demonstrated that in the paired treatment-naïve HNSCC tumor and plasma samples ( $N = 20$ ), PEX *HLA-E* mRNA (a non-survivor-predicting marker) was positively correlated with overexpression of HLA-E protein ( $P = 0.0191$ ) and the dense population of tumor-infiltrating NK cells ( $P = 0.024$ ) in the corresponding tumor, suggesting that the HLA-E-NKG2A immune checkpoint may inhibit the antitumor effect of PD-1blockade.

**Conclusion:** The PEX mRNA signature could be useful as a companion diagnostic of nivolumab. The combination of an anti-NKG2A antibody (i.e., monalizumab) and nivolumab may serve as a treatment option for non-survivors predicted by a RT-qPCR-based pre-treatment measurement of PEX mRNAs.

#### KEYWORDS

nivolumab, head and neck cancer, biomarker, exosome, HLA-E

## Introduction

The emergence of immune checkpoint inhibitors (ICIs), especially those blocking programmed death-1 (PD-1), such as nivolumab or pembrolizumab, has had a substantial impact on the treatment of patients with recurrent or metastatic (RM) head and neck squamous cell carcinoma (HNSCC) (1). The CheckMate 141 study revealed that nivolumab treatments for selected patients achieved a long-term survival of >2 years for selected patients (2, 3), an unexpected achievement compared with conventional chemotherapeutic regimens. However, only 16.9% of patients experience this long-term survival (3); therefore, a reliable biomarker urgently needs to be established to address socioeconomic issues (4), and more importantly, an effective therapeutic strategy for a majority of non-survivors who don't benefit from nivolumab administration needs to be developed.

The prognostic and predictive ICI biomarkers has been developed by the use of tissue sample-based methods including measurement of PD-L1 expression to determine the tumor proportion score (TPS) or combined positive score (CPS), tumor mutation burden, microsatellite instability, and interferon (IFN)- $\gamma$ -related signatures (5-8). Overall, these indicators are utilized as a biomarker of pembrolizumab with limited clinical efficacy. In addition, these high cost, labor intensive, and time-consuming methods have insufficient accuracy for the response prediction of nivolumab and, more importantly, are not suitable to timely monitor the ever-changing tumor immune-microenvironment (TIME) of patients. It is necessary to establish a rapid and reliable biopsy-free prognostic biomarker (e.g., a biomarker that can be analyzed in blood) for nivolumab. In this context, exosome mRNA has attracted our attention. Exosomes are small-size (30-150 nm) extracellular vesicles secreted by a variety of cells, including cancer cells (9). Accumulating evidence

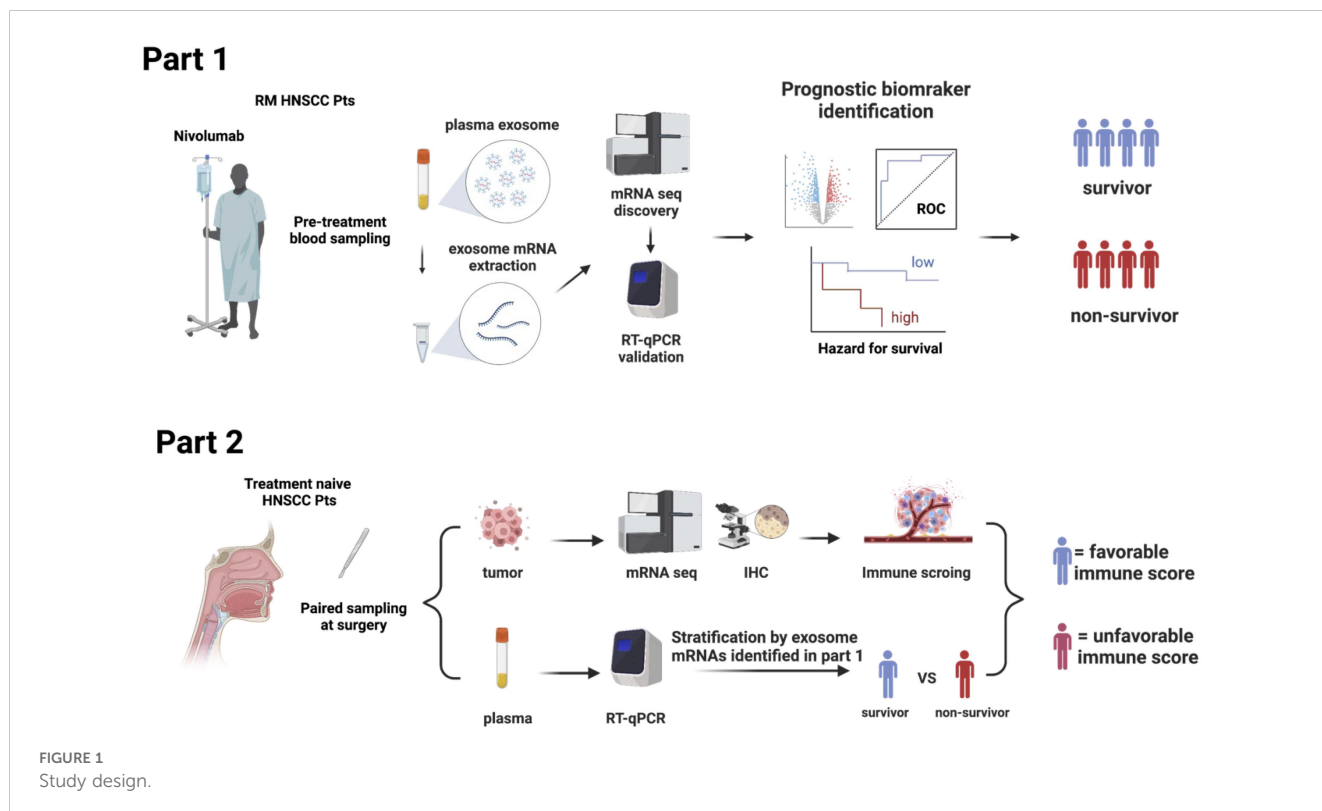
indicates that exosomes function as cargos of biological information (i.e., proteins, lipids, DNAs, and RNAs), and significantly affect the milieu and physiological functions of the recipient cells in a context-dependent manner. Notably, exosome mRNAs are transcribed and function in the recipient cells (10). Exosome-mediated-cross-talks between cancer cells and the extracellular matrix and normal cells therein (e.g., immune cells) promote a tumor-specific microenvironment that is advantageous for cancer cells to proliferate, survive, migrate, metastasize, and escape from immune surveillance (10). A recent milestone study demonstrated that exosomes secreted from *TP53*-mutated cancer cells can reprogram neurons into a cancer-promoting phenotype in HNSCC (11). The immune-suppressive effects of exosomes have also been confirmed in a series of HNSCC studies (12, 13). Thus, it is highly expected that the TIME of RM HNSCC, which regulates the response to nivolumab, can be assessed based on the plasma exosome (PEX) status. Due to the technological advancements, quantitative isolation of exosome mRNA from human samples (e.g., blood and urine) is feasible using commercially available high-throughput extraction kits in a couple of days with low cost (14, 15). Therefore, we designed a multicentric prospective study to identify a PEX mRNA signature, which is measurable in clinical practice by reverse transcription-quantitative polymerase chain reaction (RT-qPCR). The main aim of this study is to establish a companion diagnostic for nivolumab that accurately predicts non-survivors and provides a clue for the development of a novel therapeutic strategy for non-survivors.

## Methods

### Study design

The BIONEXT study is composed of the following two parts (Figure 1).

Part 1: This part included patients with RM HNSCC patients who were treated with nivolumab. Inclusion criteria were age  $\geq 20$  years; history of platinum agent administration; pathologically confirmed SCC of the nasal cavity, paranasal sinus, nasopharynx, oropharynx, oral cavity, hypopharynx, or larynx that was recurrent or metastatic and not curable by local therapy; an Eastern Cooperative Oncology Group (ECOG) performance status score of 0 or 1; and at least one tumor lesion measurable per Response Evaluation Criteria in Solid Tumors (RECIST) version 1.1 demonstrated by computed tomography imaging within 28 days of registration. The exclusion criteria were history of ICI therapy or any kind of immunotherapy; and active synchronous or metachronous (within 5 years) cancers except for the carcinoma *in situ* (CIS) and early esophageal cancer curable by endoscopic resection. Enrolled patients were treated with nivolumab (240 mg every 2 weeks or 480 mg every 4 weeks), and their responses were evaluated every 8 weeks until progressive disease (PD) was detected. Clinical data were collected through the Viedec4 electronic data capture system constructed and maintained by the Clinical Research Support Center (CRoS) Kyushu. The endpoint of this study was the identification of a PEX mRNA signature that could segregate non-survivors from long-term (> 2-year) survivors.



Pretreatment plasma samples (5 mL), collected from peripheral blood, were preserved at  $-80^{\circ}\text{C}$  until assays. Selected pilot samples were subjected to comprehensive RNA-seq analysis for the discovery of candidate PEX mRNA markers, and then the performance of these markers for prognosis prediction was validated by RT-qPCR assays in the entire cohort. All assays were conducted in compliance with the minimal information for studies of extracellular vesicle 2018 protocol (15) in the laboratory of Showa Denko Materials America under strict quality and quantity control anticipating future practical use as a companion diagnostic.

Part 2: This part was designed to confirm that the specific PEX mRNA signature could indeed reflect the TIME of the HNSCC tumors in the identical patient and moreover to elucidate the mechanism of action canceling the effects of nivolumab in non-survivors. Paired tumor and plasma samples were collected from 20 treatment-naïve patients who underwent radical surgery at the National Kyushu Cancer Center. Respective frozen and formalin-fixed paraffin-embedded (FFPE) tumor samples were subjected to mRNA-seq and immunohistochemistry (IHC) to score TIME. Concurrently, the PEX mRNA expression profile of the same patient was evaluated by RT-qPCR in reference to the prognostic biomarker genes established in part 1. Then, patients were stratified into two groups (survivor vs non-survivor signature). Comparing these two cohorts, the TIME score and the biological implication of PEX mRNA signature were investigated.

This study was approved by the Institutional Review Board of the National Kyushu Cancer Center (2019-024), and written informed consent was obtained from all patients before enrolment. This study is registered to the UMIN Clinical Trial Registry: UMIN000037029.

## Sample collection

Blood samples, taken within 28 days before nivolumab administration, were immediately centrifuged at 1100xg for 10 minutes and 5 ml of plasma samples were dispensed and snap-frozen at  $-80^{\circ}\text{C}$ . Sample collection, preservation, and shipment to Showa Denko America were performed by the SRL Inc. (Tokyo, Japan) under restrict quality and temperature management.

## PEX mRNA isolation and sequencing

PEXs were quantitatively isolated from plasma using a high throughput ExoComplete isolation tube kit (Showa Denko Materials, Tokyo, Japan), and total RNA was isolated with a MagMax Total Nucleic Acid Isolation Kit (Thermo Fisher, CA) as previously described unless otherwise noted (14). cDNA libraries were prepared using a TruSeq mRNA stranded library kit (Illumina, CA) and sequenced by paired-end read sequencing on a NovaSeq 6000 (Illumina, CA). The obtained raw reads were mapped against the human genome (GRCh38.p13) by hitsat2 and the read counts were obtained by featureCount on a Linux workstation. Differential gene expression analysis was performed by edgeR.

## PEX mRNA RT-qPCR assay

PEX mRNA isolation was conducted as described above. cDNA was synthesized with qScript XLT cDNA SuperMix (Quantabio, MA, USA) following the manufacturer's protocol. qPCR was performed with SsoAdvanced Universal SYBR Green Supermix (Bio-Rad, CA, USA) in a ViiA 7 Real-Time PCR System (Thermo Fisher Scientific, CA, USA) with the following protocol:  $95^{\circ}\text{C}$  for 10 min, followed by 40 cycles of  $95^{\circ}\text{C}$  for 30 s and  $65^{\circ}\text{C}$  for 1 min and a melting curve analysis. The primer sequences are shown in **Supplementary Table S1**. Threshold cycle (Ct) values of the marker candidates were normalized to that of the reference gene (*GAPDH*) using the delta Ct method.

## IHC

Human leukocyte antigen E (HLA-E) and programmed death ligand 1 (PD-L1) protein expression levels in the FFPE tumor samples were analyzed using a Ventana Benchmark Ultra slide processor using antibodies against HLA-E (MEM-E/02; Sant Cruz Biotechnology, Inc.) and PD-L1(22C3; PharmDx). The CPS was calculated according to the standard method (5). HLA-E tumor expression was interpreted as strong when more than half of tumor cells was positive, whereas as low when less than half of cells were positive.

## RNA-seq of primary tumor tissues and scoring of the TIME

RNA extracted from the 17 primary tumor tissues was sequenced on a DNBSEQ-G400 sequencer at Beijing Genomics Institutions (Shenzhen, China). The sequenced reads were aligned to the human reference GRCh38 genome by STAR v2.7.9a with Gencode v38 annotations using the supercomputing system SHIROKANE (University of Tokyo). Transcript-per-million (TPM)-normalized read count tables were generated by RSEM. Downstream analyses were conducted using R v4.1.1. (The R Foundation for Statistical Computing). The IFN-g-signature (the original 6 genes and an expanded 18 genes signature) and the proportions of immune cells in primary tumor tissues were estimated according to the methods in previous reports (6, 7) and CIBERSORTx (<https://cibersortx.stanford.edu/>) (16). The 17 cases were divided into two groups according to *HLA-E* expression levels based on the median value. The difference in the IFN-g-signature and the proportions of immune cells between the *HLA-E* high and low groups were examined by Mann-Whitney U tests. The correlations of the detected marker genes between tissue and PEX-mRNA were examined by Pearson correlation tests.

## Statistics

Data analysis was performed using R version 4.1.1 unless otherwise noted. Statistical significance was determined by a *p*-

value of < 5% derived from ANOVA or Welch's t test. The performance of the marker candidates was evaluated by the AUC of ROC analysis by R package pROC. The optimum threshold was obtained based on the point of the ROC curve nearest to the top-left corner and used to calculate sensitivity, specificity, positive predictive value (ppv), and negative predictive value (npv) to characterize the performance of marker candidates. Sparse logistic regression was also employed to further validate the predictive values of the biomarkers (17). Survival endpoints used to analyze the candidate biomarkers were visualized using Kaplan-Meier analysis. The log-rank test was applied to test the differences among survival curves. Cox proportional hazards regression models were used to calculate the HR.

## Results

### Enrollment and clinical outcomes

Part 1 of the study enrolled 111 patients from July 7, 2019, to December 31, 2020, and the clinical data were collected and monitored until July 2022 by CReS Kyushu. Seven patients were excluded due to screening ( $N = 6$ ) and sampling ( $N = 1$ ) errors; therefore, the samples and clinical records of 104 patients were utilized for the biomarker assay and survival curve generation. Among them, 7 (6.7%) patients demonstrated a complete response (CR), 12 (12%) had a partial response (PR), 25 (24%) had stable disease (SD), 55 (53%) had progressive disease (PD), and 5 (4.8%) were not evaluated (NE) due to rapid tumor progression. These response rates were similar to those seen in the real world large scale data in Japan (18). The characteristics of the 104 patients are shown in [Supplementary Table S2](#).

### Candidate BOR-predicting PEX mRNA discovery

Based on the previous findings that the survival of patients treated by ICI could be stratified by best overall response (BOR) (19), we adopted a standard strategy to initially develop a BOR-predicting biomarker employing receiver operating characteristic (ROC) curve analyses and then to apply this biomarker to prognostic prediction by calculating cumulative survival rates and hazard ratios (HRs) between the marker-selected (i.e., high vs low) cohorts. In preparation for BOR-predicting biomarker exploration, we confirmed the accuracy of BOR for survival prediction in the current cohort ( $N = 104$ ). As shown in [Figures 2A, B](#), the overall survival (OS) rates of patients were well stratified in accordance with BOR; no patients were lost in the CR arm, while extremely poor prognosis was observed in patients with NE, who experienced rapid tumor progression before the first evaluation ([Figure 2A](#)). Consequently, a substantial difference was found between the curves of responders ( $N = 19$ ) and non-responders ( $N = 85$ ) for 2-year OS (93.3% vs. 12.3%, Log-rank test  $P = 0.00000339$ ; HR: 0.04; 95% confidence interval [CI]: 0.0055-0.293,  $P = 0.0015079$ ) ([Figure 2B](#)). However, not only responder (CR+PR), non-

responder patients demonstrated long-survival; SD patients revealed a 48.7% of OS at 20 months and PD patients a 20.7% of OS at 2 years ([Figure 2A](#)), reflecting the fact that a certain portion of patients show durable responses to salvage chemotherapy beyond PD following nivolumab (20). Given that our main goal is to establish an accurate non-survivor-predicting biomarker, these beyond-PD survivors pose a conundrum. This is because, when response-predicting (i.e., responder vs non-responder) biomarkers are applied to survival analyses in this setting, a responder-predicting biomarker with high specificity (score low patients = responders) keeps its power as a survivor-predicting prognostic biomarker, whereas a non-responder predicting biomarker with high sensitivity (score high patients = non-responders) loses its power as a non-survivor-predicting prognostic biomarker, mispredicting these beyond-PD survivors as non-survivors. Keeping this critical point in mind, we proceeded to the identification of a BOR-predicting PEX mRNA biomarker. We cumulatively collected PEX mRNA sequencing data employing 17 plasma samples of initial phase patients (PR: 6; SD: 5; and PD: 6) when their responses were determined as of November 2020. It is of note that these 6 PR patients were > 2-year survivors (i.e., good responders). Then, we selected candidate BOR-predicting PEX mRNA, adopting a less restricted marker-selecting condition not confining the comparisons of groups between responders and non-responders, thus if they met one of the following criteria: 1) genes that were differentially expressed among the BOR categories (PR vs PD, PR vs SD/PD, and PR/SD vs PD) ( $P < 0.05$ ), 2) genes with  $|\log(\text{fold change})| > 1.5$ , 3) genes with high area under the curve (AUC) values ( $> 0.7$ ) in the ROC analyses for detection of PR vs PD, PR/SD vs PD (AUC1) and PR vs SD/PD (AUC2), or 4) genes identified as potential biomarkers in previous ICI studies (6, 8, 21, 22) or with high  $|\log(\text{fold change})|$  values in the present study. With these less broad criteria, the top 20 genes, *TAF4B*, *TESK2*, *MFSD8*, *RABL2B*, *ZNF480*, *FAM76A*, *TGIF1*, *TNFRSF13C*, *CTSW*, *LOC283788*, *SLC25A13*, *HLA-DQA1*, *COL10A1*, *MPIG6B*, *RPL23AP7*, *MSH2*, *CD3D*, *TCF7*, *HLA-E*, and *HLA-DRA* were selected as candidate BOR-predicting biomarkers for further analyses ([Figure 2C](#); [Supplementary Table S3](#)).

### Response-predicting PEX mRNA biomarker identification

Employing these candidate BOR-predicting PEX mRNAs, their powers for response prediction (i.e., responder vs non-responder) were investigated by RT-qPCR assays in the entire cohort ( $N = 104$ ). To normalize the PEX mRNA data, two representative reference genes, *ACTB* and *GAPDH*, were added to assays. Interestingly, they demonstrated significantly (*ACTB*,  $P < 0.001$ ; *GAPDH*,  $P < 0.05$ ) higher expression (i.e., raw threshold cycle value) in the non-responder than in the responder. Assuming that these increases may reflect the vigorous total exosome production from aggressive cancer cells as confirmed in previous studies (10), we adopted *ACTB*, which had a greater difference, as one of the candidate biomarker PEX mRNAs, and used *GAPDH* as the reference gene. We then compared the expression levels of *GAPDH*-normalized 21

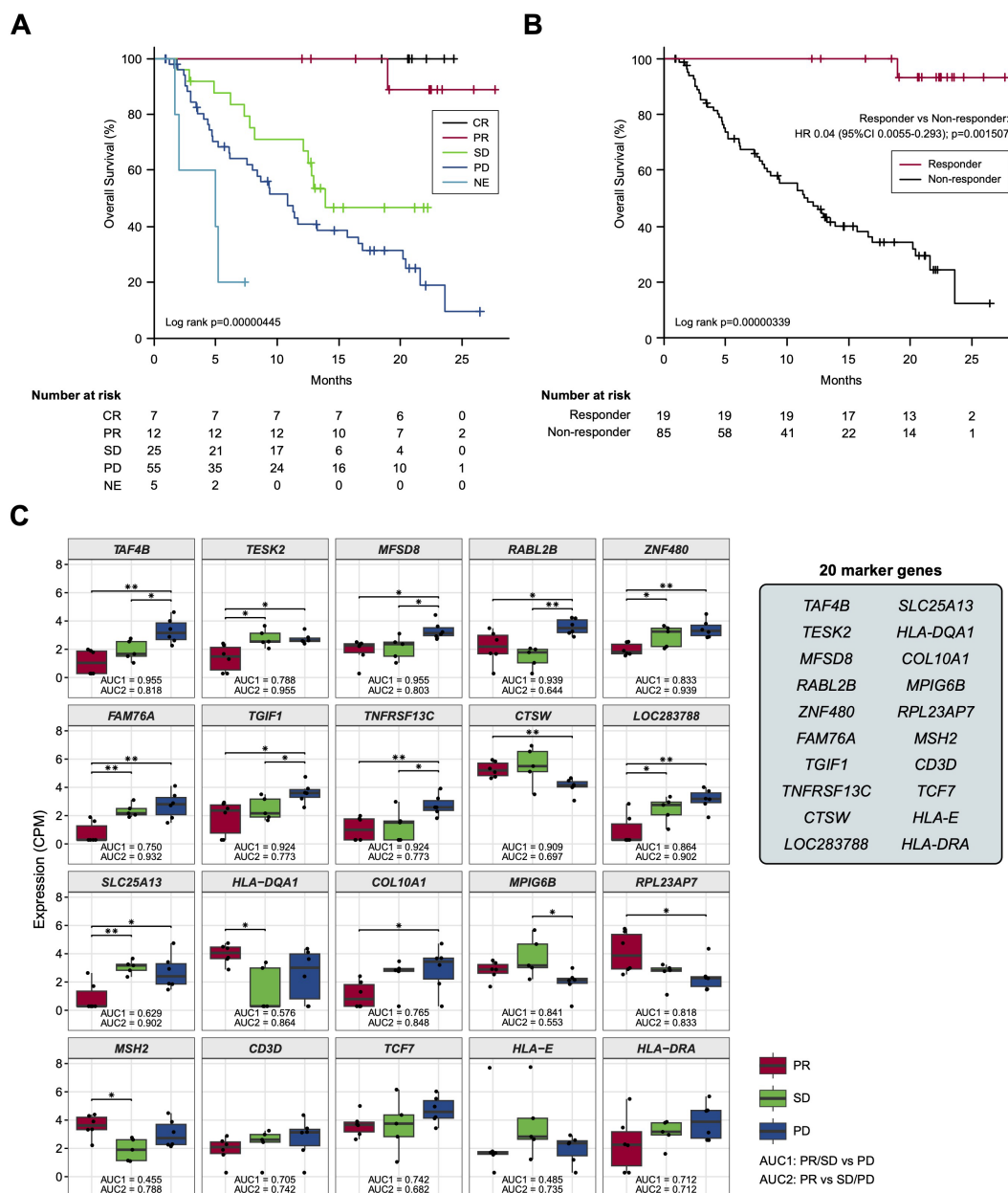


FIGURE 2 (A, B) Kaplan-Meier curves representing the overall survival of patients classified according to the best overall response. (C) Box plots representing the expression levels of 20 candidate biomarker genes in patients stratified according to the best overall response. CR, complete response; PR, partial response; SD, stable disease; PD, progressive disease; NE, not evaluated. (\*)  $P < 0.05$ ; (\*\*)  $P < 0.005$ .

PEX mRNAs between responders and non-responders and their response-predicting powers were measured by the values of AUC in the ROC curve analyses and their optima thresholds were determined by the point nearest to the top-left corner on the ROC curve. The top 6 genes with the high AUCs, *HLA-E*, *ACTB*, *MPIG6B*, *RABL2B*, *TNFRSF13C*, and *ZNF480*, were selected as putative response-predicting biomarkers (Supplementary Table S4). PEX mRNAs that were increased in the non-responders (*HLA-E*, *ACTB*, *MPIG6B* and *TNFRSF13C*) were considered as non-responder-predicting markers, while those that were increased in the responders (*RABL2B*, and *ZNF480*) were considered as responder-predicting markers (Figure 3A). Of note, the *GAPDH*-normalized *ACTB* PEX

mRNA remained significantly higher in non-responders, supporting our hypothesis. The AUC of these PEX mRNAs ranged from 0.593 to 0.729. For comparison, we calculated the AUC of the neutrophil-to-lymphocyte ratio (NLR), a proposed non-responder-predicting biomarker of ICI (23, 24), and found it was 0.591 (Supplementary Table S4; Figure 3A). The performance of individual PEX mRNAs was better than that of the NLR, but the values were not sufficiently high for clinical use. We then employed a simple algorithm to develop a better signature for response prediction by the combination of multiple PEX mRNA markers and the NLR. With the intent to generate non-responder-predicting combinations, we assigned 1 point if the expression of a non-responder-predicting gene or NLR

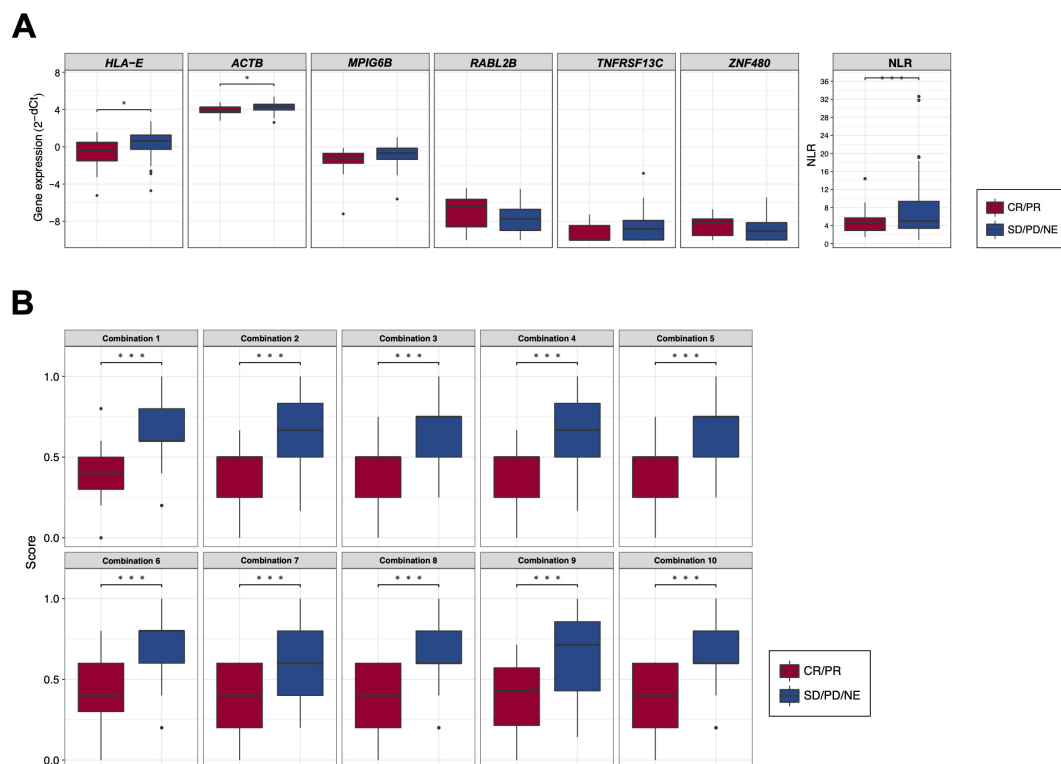


FIGURE 3

(A) Box plots comparing the expression levels of response-predicting biomarker genes and the neutrophil-to-lymphocyte ratios (NLR) between responders (CR/PR) and non-responders (SD/PD/NE). (B) Box plots comparing the scores of combinations calculated by biomarker genes and the NLR between responders (CR/PR) and non-responders (SD/PD/NE). (\*)  $P < 0.05$ ; (\*\*)  $P < 0.005$ ; (\*\*\*)  $P < 0.0005$ .

exceeded the threshold or a responder-predicting gene fall below the threshold using the best threshold value (i.e., the point of the highest sensitivity and specificity) of each marker determined by the ROC curve analysis (Supplementary Table S4), and the points were averaged for various marker combinations. The score ranged between 0 and 1, and a score of 0 indicated that no marker in the combination predicted a non-responder, while a score of 1 indicated that all markers in the combination predicted a non-responder. To obtain the best combination of markers, we tested all the possible combinations of the top 6 markers and the NLR and identified the top 10 combinations with higher AUCs (ranging from 0.793 to 0.812) (Table 1; Figure 3B). In the comparison of responders and non-responders, the scores of these combinations demonstrated more significant differences ( $P < 0.0005$ ) (Figure 3B) than the mean expression of individual 6 PEX mRNAs and NLR, in which only *HLA-E*, *ACTB* ( $P < 0.05$ ) and NLR ( $P < 0.005$ ) demonstrated significant differences (Figure 3A). Notably, all the top 10 combinations included *HLA-E*, which may suggest its importance for response prediction (Table 1).

## Prognostic biomarker identification

In our final assay, we investigated whether these non-responder-predicting combinations can serve as prognostic

biomarkers for the prediction of non-survivors. Kaplan-Meier curves of patients were generated according to the thresholds of combinations 1-10 (Table 1). In combination 1, 2, 4, 7, 9, and 10, patients with high non-responder scores (above the threshold) demonstrated significantly ( $P = 0.0002348-0.0238$ ) higher HRs (2.09-2.878) (Figure 4A). Strikingly, in the most promising (i.e., high HR) combinations (9 and 10), the OS of the patients with high non-responder scores demonstrated a sharp drop towards 0% at 2 years (Figure 4B), while that of patients with low non-responder scores demonstrated an approximately 60% 2-year OS and a tendency to plateau after 20 months. Considering the highest HR and the lowest  $P$  value, we determined to adopt the combination 9 as a prognostic biomarker of nivolumab.

## Correlation of prognostic biomarker combinations with the TIME

In part 1 of our study, we identified a prognostic biomarker combination (*HLA-E*, *ACTB*, *MPIG6B*, *RABL2B*, *TNFRSF13C*, *ZNF480* and NLR) that could precisely predict non-survivors treated with nivolumab. We then proceeded to part 2 of the study to confirm that the combination of 6 PEX mRNAs and NLR indeed reflect the TIME and, more importantly, to find a biological clue for the development of novel strategies for non-survivors (Figure 1).

TABLE 1 Candidate response-predicting combinations (assessed in responder vs non-responder groups).

|         | AUC                 | Threshold | Sensitivity | Specificity | ppv   | npv   | Markers                                       |
|---------|---------------------|-----------|-------------|-------------|-------|-------|---|
| Comb 1  | 0.812 (0.716-0.907) | 0.5       | 0.765       | 0.737       | 0.929 | 0.412 | HLA-E RABL2B TNFRSF13C ZNF480 NLR             |
| Comb 2  | 0.809 (0.722-0.896) | 0.583     | 0.635       | 0.895       | 0.964 | 0.354 | HLA-E ACTB RABL2B TNFRSF13C ZNF480 NLR        |
| Comb 3  | 0.803 (0.714-0.893) | 0.625     | 0.635       | 0.895       | 0.964 | 0.354 | HLA-E RABL2B TNFRSF13C ZNF480                 |
| Comb 4  | 0.801 (0.713-0.890) | 0.583     | 0.635       | 0.895       | 0.964 | 0.354 | HLA-E MPIG6B RABL2B TNFRSF13C ZNF480 NLR      |
| Comb 5  | 0.796 (0.702-0.890) | 0.625     | 0.576       | 0.895       | 0.961 | 0.321 | HLA-E TNFRSF13C ZNF480 NLR                    |
| Comb 6  | 0.796 (0.702-0.890) | 0.5       | 0.765       | 0.632       | 0.903 | 0.375 | HLA-E ACTB RABL2B TNFRSF13C ZNF480            |
| Comb 7  | 0.795 (0.705-0.885) | 0.5       | 0.729       | 0.632       | 0.899 | 0.343 | HLA-E MPIG6B TNFRSF13C ZNF480 NLR             |
| Comb 8  | 0.795 (0.703-0.887) | 0.5       | 0.753       | 0.579       | 0.889 | 0.344 | HLA-E ACTB TNFRSF13C ZNF480 NLR               |
| Comb 9  | 0.794 (0.700-0.887) | 0.643     | 0.576       | 0.947       | 0.98  | 0.333 | HLA-E ACTB MPIG6B RABL2B TNFRSF13C ZNF480 NLR |
| Comb 10 | 0.793 (0.700-0.886) | 0.5       | 0.753       | 0.632       | 0.901 | 0.364 | HLA-E ACTB RABL2B TNFRSF13C NLR               |

AUC, area under curve; ppv, positive predictive value; npv, negative predictive value.

For part 2, 20 paired blood, plasma and tumor samples were collected from the treatment-naïve HNSCC patients who underwent radical surgery at National Kyusyu Cancer Center. This is mainly because it is often difficult to obtain appropriate tumor samples from the patients with R/M HNSCC. Blood samples were used for the measurement of NLR. Plasma samples were subjected to PEX mRNA assay and tumor samples were to RNA-seq and IHC. Sufficient tissue amounts for RNA-seq were not obtained for 3 frozen tumor samples; thus, 17 tumor samples were subjected to the mRNA analyses, 20 tumor samples were subjected to the IHC analysis, and 20 plasma samples for PEX mRNA assay. We first measured the expression levels of *GADPH*-normalized 6 PEX mRNAs by RT-qPCR and the levels of mRNAs in the corresponding tumors by RNA-seq to examine their correlations. Consistent with the previous finding that only specific genes demonstrated significant correlations (25), PEX *HLA-E* mRNA showed a near-significant ( $P = 0.052$ ) correlation with tumor *HLA-E* mRNA among the 6 genes (Figure 5A). In view of this positive tendency, we compared the expression levels of PEX *HLA-E* mRNA and HLA-E protein in the tumors and found a significant association ( $P = 0.0191$ ) (Figure 5C). Collectively, the high PEX *HLA-E* mRNA expression appears to reflect the high *HLA-E* mRNA transcription and protein translation in the corresponding tumor. We then attempted to stratify the 20 patients into score high candidate non-survivors and score low candidate survivors based on the biomarker combination 9 established in part 1 of the study (Table 1; Figure 1A). However, interestingly, all 20 patients were grouped with survivor signature, because in the blood and plasma samples obtained from the treatment-naïve patients the NLR and the mean PEX mRNA expression levels of 6 PEX mRNAs except for *TNFRSF13C* indicated favorable response patterns compared to the RM samples (Figure 5B); *HLA-E*, *ACTB*, and *MPIG6B* (non-responder genes) were lower and *RABL2B* and *ZNF480* (responder genes) were higher. This result is consistent with the fact that the TIME of treatment-naïve tumor is more tumor-eliminating compared to the exhausted TIME of RM tumor, warranting the efficacy of this biomarker as a monitor of the TIME. Given the prominent role of HLA-E repeatedly identified

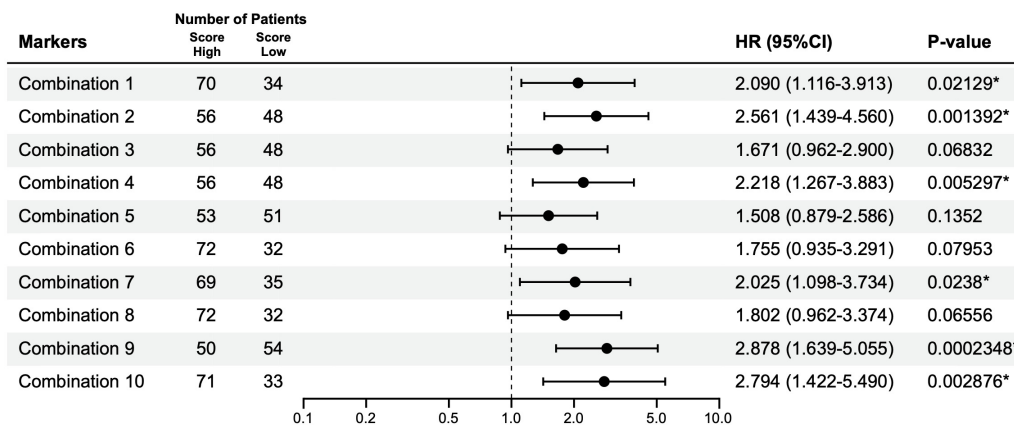
in the present study and its importance as a target of immunotherapy (i.e., therapies targeting the HLA-E-NKG2A immune checkpoint) (26, 27), we alternatively utilized the mean value of PEX *HLA-E* mRNA to stratify the 20 patients. We compared the status of immune parameters (PD-L1 CPS score, IFN- $\gamma$ -related signature score, and CIBERSORT-derived infiltrating immune cell levels) (6, 7, 16) between PEX *HLA-E* mRNA high ( $N = 10$ ) and low ( $N = 10$ ) patients. The CPS ( $P = 0.6242$ ) and IFN- $\gamma$ -related signature ( $P = 0.1802$ ) did not show significant correlations with the levels of PEX *HLA-E* mRNA. However, the number of activated natural killer (NK) cells determined by CIBERSORT were significantly ( $P = 0.024$ ) abundant in the tumors of patients with high PEX *HLA-E* mRNA (Figure 5D). It is known that HNSCC is the most immune-infiltrating cancer types across the solid tumors (28) and these tumor-infiltrating NK cells and CD8<sup>+</sup> cytotoxic T lymphocytes (CTL) strongly express NKG2A and PD-1 (27). Considering the positive correlation of PEX *HLA-E* mRNA and HLA-E protein expression confirmed above, the effects of PD-1 blockade by nivolumab may be canceled by HLA-E-NKG2A check point in patients with high PEX *HLA-E* mRNA, as illustrated in Figure 5E. Thus, the combination of clinically usable anti-NKG2A antibody (i.e., monalizumab) and nivolumab may be useful for the candidate non-survivors predicted by the pre-treatment biomarker combination indicating high PEX *HLA-E* mRNA.

## Discussion

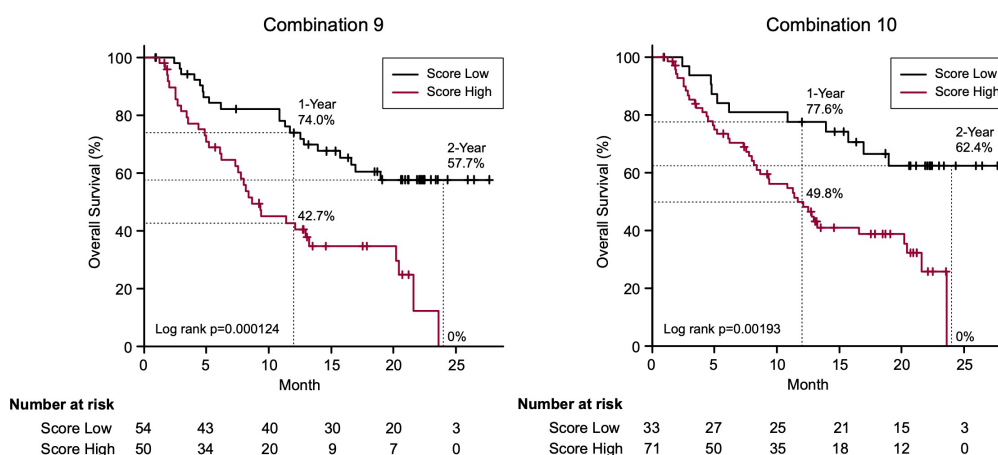
To the best of our knowledge, this is the first prospective study to demonstrate the feasibility of a single pretreatment RT-qPCR-based blood test for predicting the non-survivors with RM HNSCC treated with to nivolumab. In this study, we adopted a standard strategy to apply response-predicting biomarkers identified by the ROC curve to the survival analyses (29). For the development of marker combination, we adopted a simple algorithm which is suitable for clinical use after confirming its credibility on a sparse logistic regression algorithm (17) (data not shown). Although the



**A**



**B**



**C**

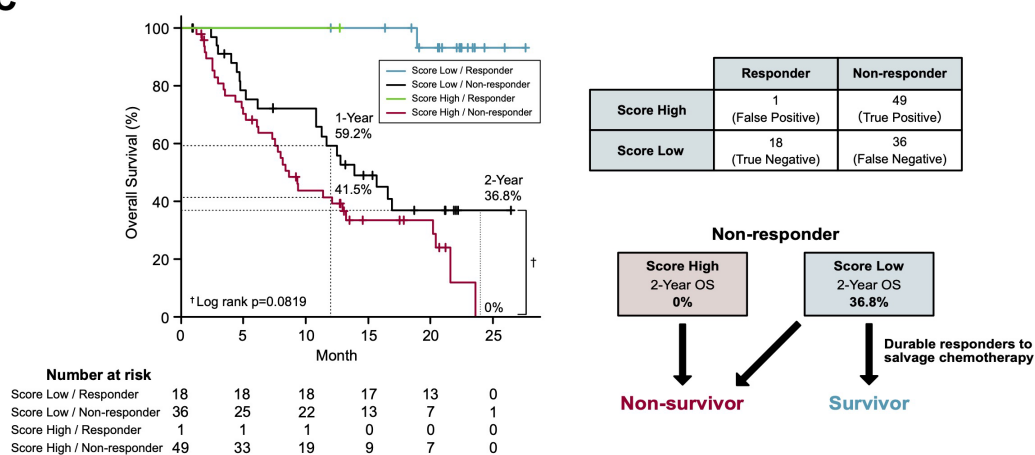


FIGURE 4

Survival prediction based on the identified biomarker combinations. (A) Forest plots representing the hazard ratios of the biomarker combinations. HR, hazard ratios; CI, confidence intervals. (B) Kaplan-Meier curves representing the overall survival of patients classified according to the score of biomarker combination (left panel, combination 9; right panel, combination 10). (C) Kaplan-Meier curves (left panel) representing the overall survival of patients classified according to the 2 x 2 contingency table (right panel). (\*)  $P < 0.05$ .

combination 9 showed a limited sensitivity (0.576) and negative predictive value (0.333) in the response prediction (Table 1), it demonstrated a strong non-survivor predicting power. To explain this mechanism, we disassembled the Kaplan-Meier curve of

combination 9 (Figure 4B) based on the distribution of patients divided in the 2 x 2 contingency table (response x combination 9 score) (Figure 4C). Strikingly, in non-responders, combination 9 score precisely segregated non-survivors in the score-high

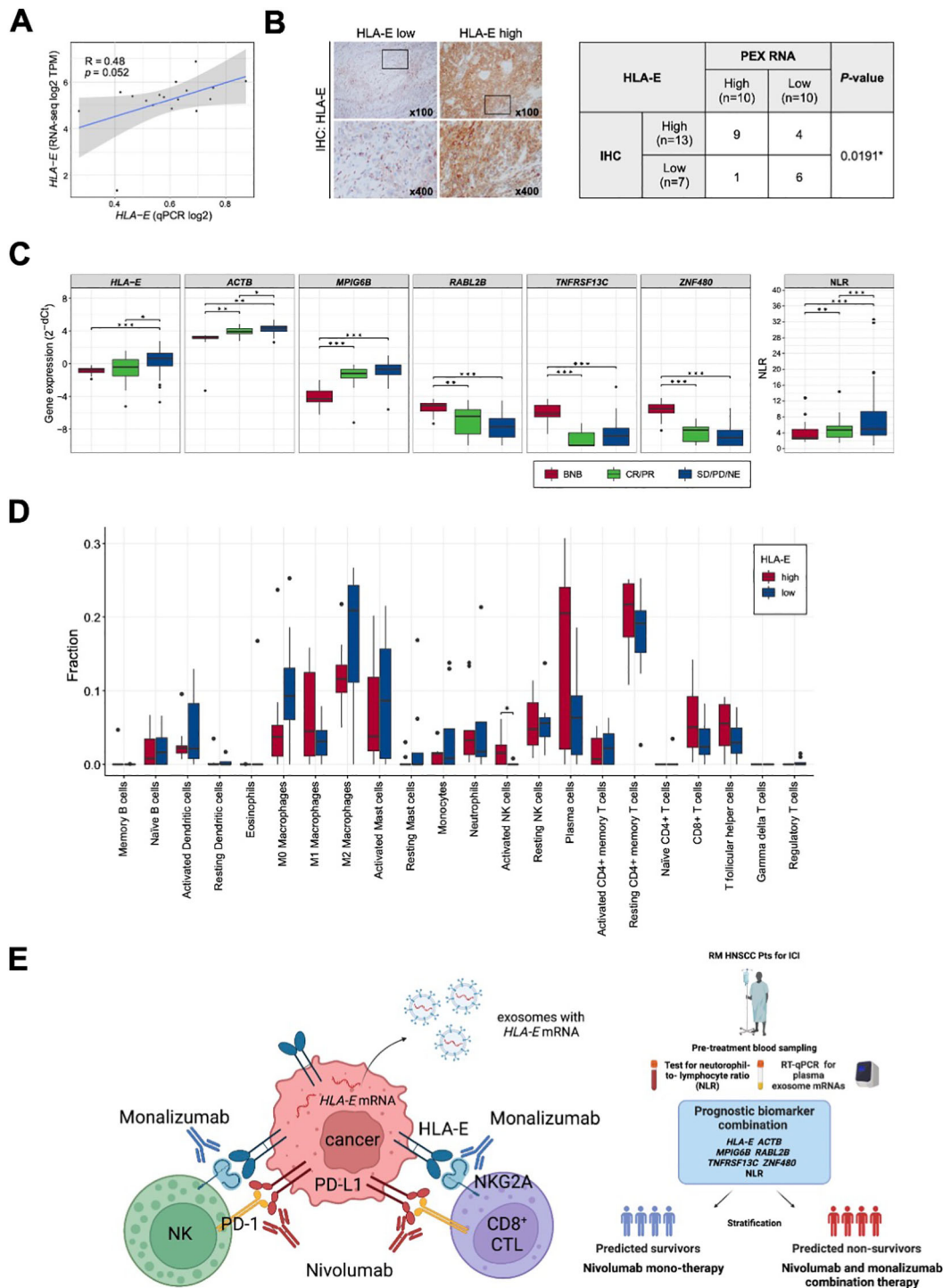


FIGURE 5

Correlation of PEX mRNA and the tumor immune microenvironment. (A) Correlation between the *HLA-E* expression levels detected by RNA-seq (vertical axis) and qPCR (horizontal axis) ( $N = 17$ ).  $R$  represents the Pearson correlation coefficient. (B) Representative images of immunohistochemistry staining for *HLA-E* in tumor tissues; *HLA-E* low (left) and *HLA-E* high (right). High-magnification images of the regions indicated by black boxes are shown. The table represents the numbers of cases and the correlation between *HLA-E* protein and *HLA-E* mRNA expression levels in PEXs ( $N = 20$ ). The  $P$ -value was calculated by Fisher's exact test. (\*)  $P < 0.05$ ; (\*\*)  $P < 0.005$ ; (\*\*\*)  $P < 0.0005$ . (C) Box plots representing the expression levels of biomarker genes detected by RT-qPCR of exosomes extracted from peripheral blood and the NLR. BNB represents the cohort of part 2 study cohort ( $N = 20$ ). CR, complete response; PR, partial response; SD, stable disease; PD, progressive disease; NE, not evaluated. (D) Box plots representing the proportion of immune cells estimated by CIBERSORTx in the primary tumor tissues ( $N = 17$ ). Patients were classified according to the expression levels of PEX *HLA-E* mRNA (*HLA-E* high,  $N = 9$ ; *HLA-E* low,  $N = 8$ ).  $P$ -value was calculated by Mann-Whitney U-tests. (\*)  $P < 0.05$ ; (\*\*)  $P < 0.005$ ; (\*\*\*)  $P < 0.0005$ . (E) Schematic summarizing of our proposed mechanism by which the effect of nivolumab is canceled in the tumor of patient with high PEX *HLA-E* mRNA (left panel) and a decision-making algorithm for patients (right panel). The high PEX mRNA level reflects the vigorous *HLA-E* protein production in cancer cells, forming *HLA-E*/*NKG2A* checkpoint with NK and *CD8*<sup>+</sup>CTL cells. In this setting, administration of nivolumab alone is not effective. Addition of an anti-*NKG2A* antibody, monalizumab, is expected to restore the cytotoxic effects of NK and CTL cells circumvented by the dual immune checkpoints.

population and exclusively separated the beyond-PD durable responders in the score-low population (2-year OS: 0% vs 36.8%, Log rank  $P = 0.0819$ , HR 1.642; 95% confidence interval 0.9335–2.887;  $P = 0.0852$ ) (Figure 4C). Consequently, a 12.3% of 2-year OS in BOR-determined non-responders ( $N = 85$ ) (Figure 2A) dropped to 0% ( $N = 50$ ) in patients with high combination 9 score (Figure 4B). The broad curation of BOR- predicting PEX mRNAs in the discovery cohort might contribute to this improvement.

Currently, an IFN- $\gamma$ -related signature (the original 6 genes and an expanded 18-gene signature), which was established as a biomarker of pembrolizumab using the tissue-based NanoString platform, is often employed (5, 8) based on its relatively high AUC of 0.75 for response prediction in RM HNSCC (6). However, the power of this biomarker remains unclear when utilized as a prognostic biomarker. The present study revealed that our liquid biomarker combinations consisting of 6 PEX mRNAs and the NLR demonstrated similar AUC of 0.794 for response-prediction and as well showed high performance as a prognostic biomarker. Considering the accuracy, speed, ease and low cost with which it can be assayed, the pretreatment measurement of NLR by routine blood test and PEX mRNA signature by RT-qPCR may be a novel companion strategy for nivolumab therapy in patients with RM HNSCC.

In addition to serving as a novel companion diagnostic, our biomarker exploration provided evidence for the development of more effective therapeutic strategies for non-survivors. The immune evasive role of HLA-E/NKG2A immune checkpoint is confirmed in a variety of cancers (26, 27, 30). In addition, increasing evidence indicates the frequent formation of dual immune checkpoints (PD-L1/PD1 and HLA-E/NKG2A) in HNSCC (27, 28), accounting for the limited effects of nivolumab. In the UPSTREM (phase II) (31) and the INTERLINK 1 (phase III) (<https://yhoo.it/3OPZbGx>) study monalizumab alone or in combination with cetuximab (an anti-EGFR antibody) failed to show clinical efficacy for RM HNSCC. It is likely that the effect of targeting one immune checkpoint is canceled by another immune checkpoint. Thus, our strategy to simultaneously target PD-1/PD-L1 and HLA-E/NKG2A immune checkpoints for biomarker-selected patients appears to be more precise and promising (Figure 5E). The safety and efficacy of the combinational administration of durvalumab (an anti-PDL-1 antibody) and monalizumab were confirmed in the Phase II lung cancer study (32). Thus, a prospective clinical study to test our strategy appears to be promising.

Unfavorable markers including *ACTB*, *MPIG6B*, *TNFRSF13C*, and the NLR, and favorable markers including *RABL2B*, and *ZNF480*, were also in our prognostic biomarker combination. The levels of PEX *ACTB* mRNA are expected to reflect the total amounts of PEX, as mentioned above, being related to proliferative activity and rapid tumor growth (10). The oncogenic and immunogenic functions of *MPIG6B* are poorly understood, but a recent study identified that this molecule is essential for the induction of megakaryocytes, which are responsible for myelofibrosis (33). *TNFRSF13C* is expressed in HNSCC tumor-infiltrating lymphocytes (34), and has been identified as an inducer of regulatory T cells in melanoma (35). The correlation of the NLR

with ICI response has been investigated in several reports, including some in HNSCC (23, 24). Overall, the reported predictive value of the pretreatment NLR alone is not sufficient, as confirmed in our study, but its utility in combination with other factors was confirmed. *RABL2B* is a small RAB GTPase. Interestingly, several members of this family of proteins (e.g., *RAB27*) are known to regulate exosome biogenesis and to promote melanoma progression (36, 37). However, the physiological and pathological functions of *RABL2B* remain unclear. The zinc finger protein, *ZNF480*, is reported to be a core transcription factor required for embryonic stem cell differentiation (38), but its oncogenic function is poorly understood. In summary, the precise roles that make these 6 PEX mRNAs good prognostic biomarkers of nivolumab should be investigated in future studies. However, given the reported and predicted functions of each gene, these molecules likely have functions in the oncogenesis and the immune system, when expressed in PEX mRNA-producing cells (e.g., cancer cells) and recipient cells (e.g., immune cells).

It is obvious that this study includes limitations such as the sample size in both part 1 and 2 and the lack of explanation about the detailed mechanisms by which several specific PEX mRNAs work as a monitor of TIME. However, it seems that the strong prognostic predictive power demonstrated by our biomarker combination compensates these limitations and encourages further validation in a larger-scale study.

In conclusion, this pilot study indicates that it might be possible to predict non-survivors following nivolumab with a single pretreatment blood test. A prospective study that examines the efficacy of simultaneous administration of nivolumab and monalizumab in the candidate non-survivors also appears to be promising.

## Data availability statement

The original contributions presented in the study are included in the article/Supplementary Material. Further inquiries can be directed to the corresponding author.

## Ethics statement

The studies involving humans were approved by Institutional Review Board of the National Kyushu Cancer Center (2019–024). The studies were conducted in accordance with the local legislation and institutional requirements. The participants provided their written informed consent to participate in this study.

## Author contributions

KS: Formal analysis, Methodology, Resources, Software, Validation, Visualization, Writing – review & editing. ST: Conceptualization, Data curation, Formal analysis, Investigation, Methodology, Project administration, Software, Supervision, Validation, Visualization,

Writing – review & editing. TMu: Conceptualization, Data curation, Formal analysis, Investigation, Methodology, Resources, Software, Supervision, Validation, Visualization, Writing – review & editing. TaN: Data curation, Formal analysis, Investigation, Methodology, Software, Validation, Visualization, Writing – review & editing. TH: Data curation, Formal analysis, Methodology, Software, Validation, Visualization, Writing – review & editing. MiM: Data curation, Writing – review & editing. KH: Data curation, Writing – review & editing. MS: Data curation, Writing – review & editing. KY: Data curation, Writing – review & editing. YU: Data curation, Writing – review & editing. ToN: Data curation, Writing – review & editing. HUR: Data curation, Writing – review & editing. TO: Data curation, Writing – review & editing. HU: Data curation, Writing – review & editing. TU: Data curation, Writing – review & editing. SK: Data curation, Writing – review & editing. KT: Data curation, Writing – review & editing. AW: Data curation, Writing – review & editing. IO: Data curation, Writing – review & editing. NM: Data curation, Writing – review & editing. SI: Data curation, Writing – review & editing. TMA: Data curation, Writing – review & editing. YA: Data curation, Writing – review & editing. NH: Data curation, Writing – review & editing. DS: Data curation, Writing – review & editing. HO: Data curation, Writing – review & editing. TA: Data curation, Writing – review & editing. TF: Data curation, Writing – review & editing. MuM: Conceptualization, Data curation, Formal analysis, Funding acquisition, Investigation, Methodology, Project administration, Resources, Software, Supervision, Validation, Visualization, Writing – original draft, Writing – review & editing.

## Funding

The author(s) declare financial support was received for the research, authorship, and/or publication of this article. This study was partly funded by JSPS KAKENHI [Grant number JP 21436707 to MuM] and Sota Memorial Fund to MuM. PEXmRNA analyses were conducted by Showa Denko America Materials. CREs Kyushu

## References

1. Le X, Ferrarotto R, Wise-Draper T, Gillison M. Evolving role of immunotherapy in recurrent metastatic head and neck cancer. *J Natl Compr Cancer Netw*. (2020) 18:899–906. doi: 10.6004/jnccn.2020.7590
2. Ferris RL, Blumenschein G Jr, Fayette J, Guigay J, Colevas AD, Licitra L, et al. Nivolumab for recurrent squamous-cell carcinoma of the head and neck. *N Engl J Med*. (2016) 375:1856–67. doi: 10.1056/NEJMoa1602252
3. Ferris RL, Blumenschein G Jr, Fayette J, Guigay J, Colevas AD, Licitra L, et al. Nivolumab vs investigator's choice in recurrent or metastatic squamous cell carcinoma of the head and neck: 2-year long-term survival update of CheckMate 141 with analyses by tumor PD-L1 expression. *Oral Oncol*. (2018) 81:45–51. doi: 10.1016/j.oraloncology.2018.04.008
4. Tringale KR, Carroll KT, Zakeri K, Sacco AG, Barnachea L, Murphy JD. Cost-effectiveness analysis of nivolumab for treatment of platinum-resistant recurrent or metastatic squamous cell carcinoma of the head and neck. *J Natl Cancer Inst*. (2017). doi: 10.1093/jnci/djx226
5. Gavrielatou N, Doumas S, Economopoulou P, Foukas PG, Psyrri A. Biomarkers for immunotherapy response in head and neck cancer. *Cancer Treat Rev*. (2020) 84:101977. doi: 10.1016/j.ctrv.2020.101977
6. Ayers M, Lunceford J, Nebozhyn M, Murphy E, Loboda A, Kaufman DR, et al. IFN-gamma-related mRNA profile predicts clinical response to PD-1 blockade. *J Clin Invest*. (2017) 127:2930–40. doi: 10.1172/JCI91190

organized sample collection and transfer, and conducted clinical data management with funding provided by Ono and Bristol-Myers Squibb. The funders had no role in the study design, data collection and analysis, decision to publish, or preparation of the manuscript.

## Acknowledgments

We thank Shoji Tokunaga (Medical Information Center, Kyushu University) for his advice on the study design (e.g., sample size) and statistical analyses and CreS Kyushu for intensive support.

## Conflict of interest

The authors declare that the research was conducted in the absence of any commercial or financial relationships that could be construed as a potential conflict of interest.

## Publisher's note

All claims expressed in this article are solely those of the authors and do not necessarily represent those of their affiliated organizations, or those of the publisher, the editors and the reviewers. Any product that may be evaluated in this article, or claim that may be made by its manufacturer, is not guaranteed or endorsed by the publisher.

## Supplementary material

The Supplementary Material for this article can be found online at: <https://www.frontiersin.org/articles/10.3389/fimmu.2024.1464419/full#supplementary-material>

7. Ott PA, Bang YJ, Piha-Paul SA, Razak ARA, Bannoun J, Soria JC, et al. T-cell-inflamed gene-expression profile, programmed death ligand 1 expression, and tumor mutational burden predict efficacy in patients treated with pembrolizumab across 20 cancers: KEYNOTE-028. *J Clin Oncol*. (2019) 37:318–27. doi: 10.1200/jco.2018.78.2276
8. Walk EE, Yohe SL, Beckman A, Schade A, Zutter MM, Pfeifer J, et al. The cancer immunotherapy biomarker testing landscape. *Arch Pathol Lab Med*. (2020) 144:706–24. doi: 10.5858/arpa.2018-0584-CP
9. Möller A, Lobb RJ. The evolving translational potential of small extracellular vesicles in cancer. *Nat Rev Cancer*. (2020) 20:697–709. doi: 10.1038/s41568-020-00299-w
10. Prieto-Vila M, Yoshioka Y, Ochiya T. Biological functions driven by mRNAs carried by extracellular vesicles in cancer. *Front Cell Dev Biol*. (2021) 9:620498. doi: 10.3389/fcell.2021.620498
11. Amit M, Takahashi H, Dragomir MP, Lindemann A, Gleber-Netto FO, Pickering CR, et al. Loss of p53 drives neuron reprogramming in head and neck cancer. *Nature*. (2020) 578:449–54. doi: 10.1038/s41586-020-1996-3
12. Whiteside TL. Exosomes and tumor-mediated immune suppression. *J Clin Invest*. (2016) 126:1216–23. doi: 10.1172/JCI81136
13. Whiteside TL, Diergaarde B, Hong CS. Tumor-derived exosomes (TEX) and their role in immuno-oncology. *Int J Mol Sci*. (2021) 22. doi: 10.3390/ijms22126234

14. Murakami T, Yamamoto CM, Akino T, Tanaka H, Fukuzawa N, Suzuki H, et al. Bladder cancer detection by urinary extracellular vesicle mRNA analysis. *Oncotarget*. (2018) 9:32810–21. doi: 10.18632/oncotarget.25998
15. Thery C, Witwer KW, Aikawa E, Alcaraz MJ, Anderson JD, Andriantsitohaina R, et al. Minimal information for studies of extracellular vesicles 2018 (MISEV2018): a position statement of the International Society for Extracellular Vesicles and update of the MISEV2014 guidelines. *J Extracell Vesicles*. (2018) 7:1535750. doi: 10.1080/20013078.2018.1535750
16. Gentles AJ, Newman AM, Liu CL, Bratman SV, Feng W, Kim D, et al. The prognostic landscape of genes and infiltrating immune cells across human cancers. *Nat Med*. (2015) 21:938–45. doi: 10.1038/nm.3909
17. Friedman J, Hastie T, Tibshirani R. Regularization paths for generalized linear models via coordinate descent. *J Stat Softw*. (2010) 33:1–22. doi: 10.18637/jss.v033.i01
18. Matsuo M, Yasumatsu R, Masuda M, Yamauchi M, Wakasaki T, Hashimoto K, et al. Five-year follow-up of patients with head and neck cancer treated with nivolumab and long-term responders for over two years. *In Vivo*. (2022) 36:1881–6. doi: 10.21873/invivo.12907
19. Licitra L, Ferris RL, Harrington KJ, Guigay J, Blumenschein G Jr., Kasper S, et al. Nivolumab vs investigator's choice (IC) in patients with recurrent or metastatic (R/M) squamous cell carcinoma of the head and neck (SCCHN): treatment effect on clinical outcomes by best overall response in checkmate 141. *Ann Oncol*. (2017) 28:377–8. doi: 10.1093/annonc/mdx374
20. Haddad R, Concha-Benavente F, Blumenschein G Jr., Fayette J, Guigay J, Colevas AD, et al. Nivolumab treatment beyond RECIST-defined progression in recurrent or metastatic squamous cell carcinoma of the head and neck in CheckMate 141: A subgroup analysis of a randomized phase 3 clinical trial. *Cancer*. (2019) 125:3208–18. doi: 10.1002/cncr.32190
21. Dominguez CX, Muller S, Keerthivasan S, Koeppen H, Hung J, Gierke S, et al. Single-cell RNA sequencing reveals stromal evolution into LRRRC15(+) myofibroblasts as a determinant of patient response to cancer immunotherapy. *Cancer Discovery*. (2020) 10:232–53. doi: 10.1158/2159-8290.CD-19-0644
22. Bai R, Lv Z, Xu D, Cui J. Predictive biomarkers for cancer immunotherapy with immune checkpoint inhibitors. *Biomark Res*. (2020) 8:34. doi: 10.1186/s40364-020-00209-0
23. Valero C, Lee M, Hoen D, Weiss K, Kelly DW, Adusumilli PS, et al. Pretreatment neutrophil-to-lymphocyte ratio and mutational burden as biomarkers of tumor response to immune checkpoint inhibitors. *Nat Commun*. (2021) 12:729. doi: 10.1038/s41467-021-20935-9
24. Wakasaki T, Yasumatsu R, Masuda M, Takeuchi T, Manako T, Matsuo M, et al. Prognostic biomarkers of salvage chemotherapy following nivolumab treatment for recurrent and/or metastatic head and neck squamous cell carcinoma. *Cancers (Basel)*. (2020) 12. doi: 10.3390/cancers12082299
25. Skog J, Wurdinger T, van Rijn S, Meijer DH, Gainche L, Sena-Esteves M, et al. Glioblastoma microvesicles transport RNA and proteins that promote tumour growth and provide diagnostic biomarkers. *Nat Cell Biol*. (2008) 10:1470–6. doi: 10.1038/ncb1800
26. Borst L, van der Burg SH, van Hall T. The NKG2A-HLA-E axis as a novel checkpoint in the tumor microenvironment. *Clin Cancer Res*. (2020) 26:5549–56. doi: 10.1158/1078-0432.CCR-19-2095
27. Andre P, Denis C, Soulas C, Bourbon-Caillet C, Lopez J, Arnoux T, et al. Anti-NKG2A mAb is a checkpoint inhibitor that promotes anti-tumor immunity by unleashing both T and NK cells. *Cell*. (2018) 175:1731–43.e13. doi: 10.1016/j.cell.2018.10.014
28. Mandal R, Senbabaoglu Y, Desrichard A, Havel JJ, Dalin MG, Riaz N, et al. The head and neck cancer immune landscape and its immunotherapeutic implications. *JCI Insight*. (2016) 1:e89829. doi: 10.1172/jci.insight.89829
29. Hatae R, Chamoto K, Kim YH, Sonomura K, Taneishi K, Kawaguchi S, et al. Combination of host immune metabolic biomarkers for the PD-1 blockade cancer immunotherapy. *JCI Insight*. (2020) 5. doi: 10.1172/jci.insight.133501
30. Sheffer M, Lowry E, Beelen N, Borah M, Amara SN, Mader CC, et al. Genome-scale screens identify factors regulating tumor cell responses to natural killer cells. *Nat Genet*. (2021) 53:1196–206. doi: 10.1038/s41588-021-00889-w
31. Galot R, Le Tourneau C, Saada-Bouزيد E, Daste A, Even C, Debruyne P, et al. A phase II study of monalizumab in patients with recurrent/metastatic squamous cell carcinoma of the head and neck: The II cohort of the EORTC-HNCG-1559 UPSTREAM trial. *Eur J Cancer*. (2021) 158:17–26. doi: 10.1016/j.ejca.2021.09.003
32. Herbst RS, Majem M, Barlesi F, Carcereny E, Chu Q, Monnet I, et al. COAST: an open-label, phase II, multidrug platform study of durvalumab alone or in combination with orelumab or monalizumab in patients with unresectable, stage III non-small-cell lung cancer. *J Clin Oncol*. (2022) Jco2200227. doi: 10.1200/jco.22.00227
33. Psaila B, Wang G, Rodriguez-Meira A, Li R, Heuston EF, Murphy L, et al. Single-cell analyses reveal megakaryocyte-biased hematopoiesis in myelofibrosis and identify mutant clone-specific targets. *Mol Cell*. (2020) 78:477–92.e8. doi: 10.1016/j.molcel.2020.04.008
34. Cillo AR, Kurten CHL, Tabib T, Qi Z, Onkar S, Wang T, et al. Immune landscape of viral- and carcinogen-driven head and neck cancer. *Immunity*. (2020) 52:183–99.e9. doi: 10.1016/j.immuni.2019.11.014
35. Zhang C, Dang D, Cong L, Sun H, Cong X. Pivotal factors associated with the immunosuppressive tumor microenvironment and melanoma metastasis. *Cancer Med*. (2021) 10:4710–20. doi: 10.1002/cam4.3963
36. Stenmark H. Rab GTPases as coordinators of vesicle traffic. *Nat Rev Mol Cell Biol*. (2009) 10:513–25. doi: 10.1038/nrm2728
37. Peinado H, Aleckovic M, Lavotshkin S, Matei I, Costa-Silva B, Moreno-Bueno G, et al. Melanoma exosomes educate bone marrow progenitor cells toward a pro-metastatic phenotype through MET. *Nat Med*. (2012) 18:883–91. doi: 10.1038/nm.2753
38. Zhang C, Li C, Yang L, Leng L, Jovic D, Wang J, et al. The dynamic changes of transcription factors during the development processes of human biparental and uniparental embryos. *Front Cell Dev Biol*. (2021) 9:709498. doi: 10.3389/fcell.2021.709498